Hindawi
Shock and Vibration
Volume 2022, Article ID 8991787, 14 pages
https://doi.org/10.1155/2022/8991787

Research Article

Noise Source Identification of the Carpet Tufting Machine Based on the Single Channel Blind Source Separation and Time-Frequency Signal Analysis

Xiaowei Sheng, Xiaoyan Fang, Yang Xu, and Yize Sun

College of Mechanical Engineering, Donghua University, Shanghai 201620, China

Correspondence should be addressed to Xiaowei Sheng; shengxw@mail.dhu.edu.cn

Received 25 June 2021; Revised 28 August 2022; Accepted 5 October 2022; Published 21 October 2022

Academic Editor: Gabriele Cazzulani

Noise source identification is the first key step to reduce the noise pressure level of the carpet tufting machine. For identifying the main noise sources of the carpet tufting machine, the single channel blind source separation (SCBSS) method is proposed to separate the acquired single channel noise, and the time-frequency signal analysis is applied to identify separated noise components. The SCBSS includes ensemble empirical mode decomposition (EEMD), improved Akaike information criterion (AIC) source number estimation and fast independent component analysis (FastICA). The separation method based on EEMD-AIC-FastICA not only overcomes traditional blind source separation problems that require enough test channel numbers, but also solves the problem that the number of virtual multichannel signals is unknown. Four independent components (ICs) are obtained after using the SCBSS. Combining the time-frequency analysis of the four ICs and the acquired vibration signals of six main components, the specific four noise sources can be identified. The four ICs correspond to the noise of needles, noise of hooks, noise of hook driven shaft, and noise of motor spindle, respectively.

1. Introduction

The carpet tufting machine is typical high-end textile machinery. According to the survey of several carpet workshops, the noise pressure level of the carpet tufting machine is generally above 85 dBA, which exceeds the national standard for noise control of industrial enterprises [1]. Textile workers may have serious physical and psychological health problems while working in a loud noise environment for a long time. In order to reduce the noise pressure level of the carpet tufting machine and set up a green manufacturing demonstration for the textile machinery, the first key step is to identify the main noise sources. The carpet tufting machine is very complicated textile machinery, which includes many noise sources. If the main noise sources can be identified, then a detail noise reduction plan can be created for specific components of the carpet tufting machine. By reducing the main noise sources, the total noise pressure level can be obviously reduced. However, the noise sources of the carpet tufting machine are coupled and mixed strongly with each other. Therefore, they are difficult to identify by using traditional signal analysis methods.

In recent years, some researchers have used blind source separation (BSS) or independent component analysis (ICA) to separate noise sources from mixed noise signals and then identify them according to their prior knowledge. For example, Chiu and Lu [2] used fast independent component analysis (FastICA) to separate the noise signal from the unusual tension signal on the yarn twist machine. Servière et al. [3] applied BSS methods to separate combustion noise and piston-slap noise in diesel engines. However, BSS and ICA methods usually require the number of acquisition channels to be greater than or equal to the number of separated sources. The carpet tufting machine usually has many intricate noise sources, and the specific number of noise sources is unknown in advance. Moreover, in practical engineering applications, due to the limitation of the experimental conditions, the acquired noise signal is usually

the single channel noise signal. Therefore, the single channel blind source separation (SCBSS) has started to be applied in noise source separation. Du et al. [4] used empirical mode decomposition and independent component analysis (EMD-ICA) to separate and identify the vibration sources of a diesel engine. Bi et al. [5] used ensemble empirical mode decomposition and robust independent component analysis (EEMD-RobustICA) to separate and identify the noise sources of gasoline engines. Yao et al. [6, 7] separate and identify the noise sources of a diesel engine by using variational mode decomposition and robust independent component analysis (VMD-RobustICA) and time-varying filtering-based empirical mode decomposition and robust independent component analysis (TVF-EMD-RobustICA) respectively. The SCBSS methods in reference [4–7] all used the adaptive mode decomposition methods first, which are the EMD method, the EEMD method, the VMD method and the TVF-EMD method, and then some typical blind source separation methods were applied. The reason of using the adaptive mode decomposition methods is to decompose the single channel signal into virtual multichannel signals. After using the adaptive mode decomposition methods, the number of virtual multichannel signals was unknown and the subjective prior knowledge was used for determining the number in reference [4–7]. Therefore, to overcome the problems above, a source number estimation method should be applied after using the adaptive mode decomposition methods. Recently, Akaike information criterion (AIC) source number estimation has been combined with the adaptive mode decomposition methods for identifying noise sources in textile machinery [8, 9]. However, the reference [8, 9] did not use any independent component analysis methods. Nonindependent decomposition components made the identification process more complicated.

Therefore, FastICA was used after EEMD and AIC, and the single channel blind source separation method (EEMD-AIC-FastICA) was applied in separating the noise sources of the carpet tufting machine. The proposed EEMD-AIC-FastICA separation method not only solved the problem of unknown source number in reference [4–7], but also overcame the problem of non-independent source signals. An acquired single channel noise signal of the carpet tufting machine was separated into several independent components (ICs) by using the EEMD-AIC-FastICA method. The ICs are the main noise sources of the carpet tufting machine. And then, by combining time-frequency analysis of the ICs and vibration signals of the main components of the carpet tufting machine, which were acquired by a fiber laser vibrometer, the specific noise sources can be identified. The main contribution of this paper is to propose a single channel blind source separation method based on the EEMD-AIC-FastICA to separate the noise sources of the carpet tufting machine. Moreover, the vibration signals of the main components of the carpet tufting machine were acquired by a fiber laser vibrometer and analyzed by time-frequency analysis. Comparing the analysis results of the ICs and the vibration signals, the specific noise sources can be obtained.

2. Related Methods

2.1. EEMD Method. EMD, which was proposed by Huang et al. in 1998 [10], may decompose a complicated signal into a series of intrinsic mode functions (IMFs) based on the local characteristic time scale of the signal. An IMF is the function that satisfies the following two conditions: (1) The number of extrema and zero-crossings must either equal or differ at most by one; (2) At any point, the mean of the upper and lower envelopes from the signal is zero.

To gain i^{th} IMF component C_i, the sifting process is shown in Figure 1. Repeat these sifting processes until the residue signal is a monotonic function. At the end of the process, a series of IMFs $C_i\,(i = 1, 2, \cdots n)$ and a residue r_n are obtained. Summing up all IMFs and the final residue r_n, the following equation is acquired.

$$X(t) = \sum_{j=1}^{n} C_j + r_n. \tag{1}$$

The IMFs include different frequency bands ranging from high to low. The frequency components contained in each frequency band are different and can change with the variation of signal $X\,(t)$. The final residue r_n represents the central tendency of signal $X\,(t)$ [11].

To overcome the mode mixing problem in EMD, EEMD was proposed by Wu and Huang [12]. The flow chart of the EEMD method is shown in Figure 2.

2.2. Improved AIC Source Number Estimation. After the signal is decomposed into several IMF components, the total energy of each IMF component and the correlation coefficient between each IMF component and the original signal are separately calculated [8]. According to the relevant feature index, all IMF components are reordered and the m most significant components are chosen to form an IMF component matrix $D = [d_1(t), d_2(t), \cdots, d_m(t)]$. The covariance matrix of D is decomposed by singular value decomposition (SVD) and m eigenvalues $\lambda_1 \geq \lambda_2 \geq \cdots \lambda_m$ corresponding to the IMF components can be obtained [13].

The noise of the carpet tufting machine is not white noise; hence, the accuracy of the AIC criterion for source number estimation is low. To solve this problem, the original method needs to be improved. The noise eigenvalues can be smoothed by diagonally loading the covariance matrix. The calibrated eigenvalue is $\mu_i = \lambda_i + \lambda_{DL}, i = 1, 2, \cdots, m$, where the loading is [8]

$$\lambda_{DL} = \sqrt{\sum_{i=1}^{m} \lambda_i}\,. \tag{2}$$

After the eigenvalue calibration, the AIC equation is

$$\mathrm{AIC}(k) = -2N(m-k)\lg\left(\frac{\prod_{i=k+1}^{m} \mu_i^{1/m-k}}{1/m - k\sum_{i=k+1}^{m}\mu_i}\right) + 2k(2m-k), \tag{3}$$

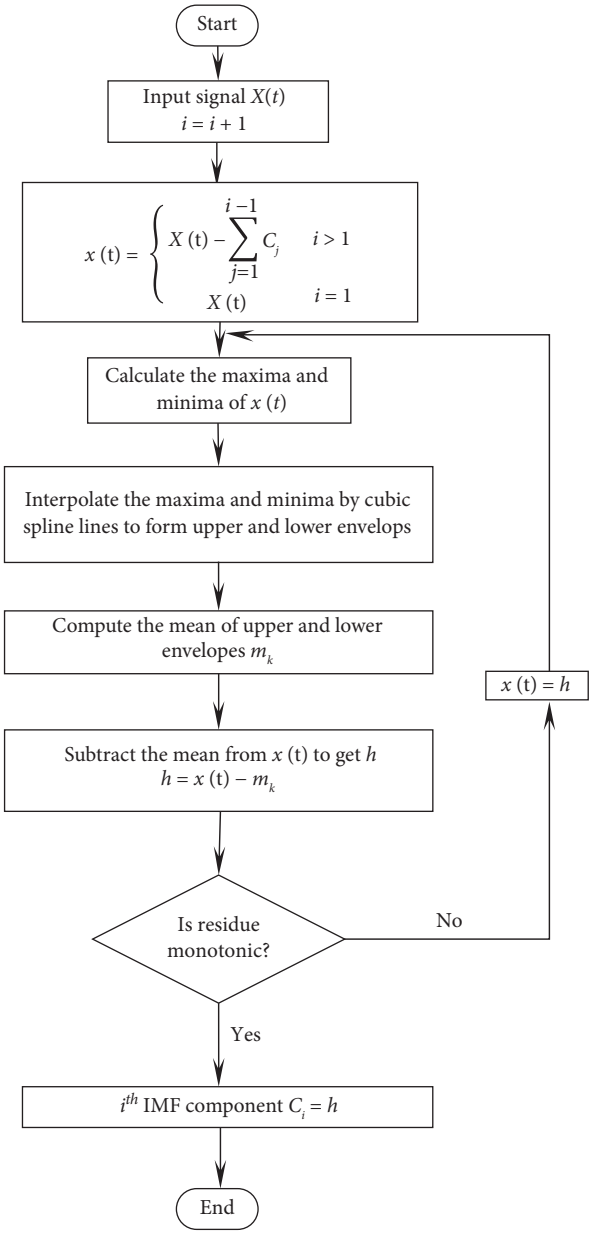

Figure 1: Sifting flow chart of i^{th} IMF component.

where N is the sample number and $k = 1, 2, \cdots, m-1$. The AIC values from $k = 1$ to m-1 are computed and the k corresponding to the smallest AIC value is the number of valid components.

2.3. FastICA Algorithm. Independent component analysis (ICA) is mainly applied in solving the blind source separation problem. The basic mathematic mixture model for ICA is as follows [5]:

$$X = AS, \tag{4}$$

where X is the mixed signal, A is the mixing matrix and S is the source signal. The ICA separation process is to recover the source signal S from the mixed signal X and it can be defined as follows:

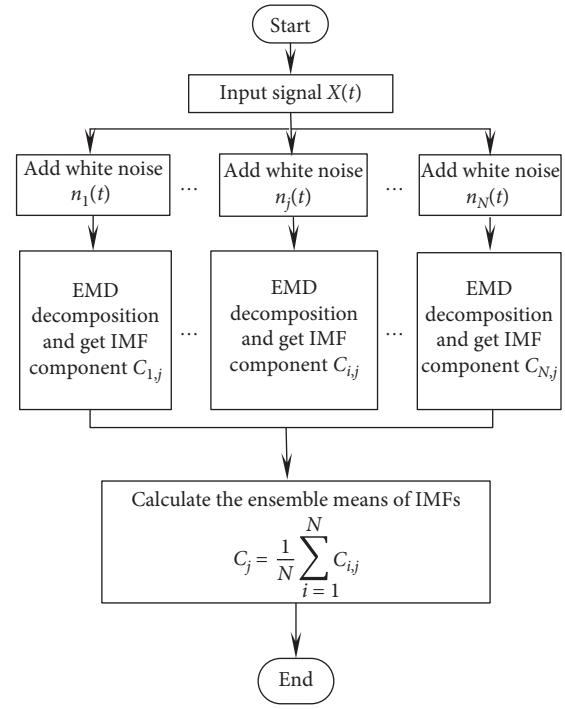

Figure 2: The flow chart of EEMD method.

$$\begin{aligned} Y &= WX = WAS, \\ W &= A^{-1}, \end{aligned} \tag{5}$$

where Y is the separated signal, W is the decoupling matrix [14].

There are several typical algorithms for ICA, such as FastICA, joint approximate diagonalization of eigenmatrices (JADE), fourth-order blind identification (FOBI) et al. Among these algorithms, FastICA has high convergence speed and satisfactory performance in a wide variety of applications and is one of the most popular iterative methods for ICA. There are three types of FastICA algorithms, which are separately based on negentropy, based on kurtosis, and based on likelihood. A fast fixed-point algorithm based on negentropy will be introduced briefly [15, 16].

Suggesting the following fixed-point iteration:

$$w = E\{zg(w^T z)\}, \tag{6}$$

where z is the whitened data, w is an initial vector, g is the derivative of nonquadratic function G. The g can be chosen from

$$\begin{aligned} g_1(y) &= \tanh(a_1 y), \\ g_2(y) &= y \exp\left(-\frac{y^2}{2}\right), \\ g_3(y) &= y^3, \end{aligned} \tag{7}$$

where $1 \le a_1 \le 2$ is some suitable constant, often taken as $a_1 = 1$.

Add w, multiplied by some constant α, on both sides of equation (6) without modifying the fixed points and get following equation.

$$(1+\alpha)w = E\{zg(w^Tz)\} + \alpha w, \tag{8}$$

where the coefficient α can be found using an approximative Newton method.

According to the Lagrange conditions, the optima of $E\{G(w^Tz)\}$ under the constraint $E\{(w^Tz)^2\} = \|w\|^2 = 1$ are obtained at points where the gradient of the Lagrangian is zero:

$$E\{zg(w^Tz)\} + \beta w = 0, \tag{9}$$

where β is a constant.

Denoting the function on the left-hand side of equation (9) by F, its gradient can be obtained as follows:

$$\frac{\partial F}{\partial w} = E\{zz^Tg'(w^Tz)\} + \beta I. \tag{10}$$

The first term of equation (10) can be approximated as follows:

$$E\{zz^Tg'(w^Tz)\} \approx E\{zz^T\}E\{g'(w^Tz)\} = E\{g'(w^Tz)\}I. \tag{11}$$

Therefore, the approximative Newton iteration can be obtained as follows:

$$w \leftarrow w - \frac{[E\{zg(w^Tz)\} + \beta w]}{[E\{g'(w^Tz)\} + \beta]}. \tag{12}$$

Multiply both sides of equation (12) by $E\{g'(w^Tz)\} + \beta$ and simplified equation can be obtained as follows:

$$w \leftarrow E\{zg(w^Tz)\} - E\{g'(w^Tz)\}w. \tag{13}$$

Equation (13) is the basic fixed-point iteration in FastICA.

2.4. Process of the Noise Source Identification of the Carpet Tufting Machine. The schematic of the noise source identification of the carpet tufting machine is illustrated in Figure 3. Because the vibration can generate the noise, noise source should have a relationship with the vibration source. The vibration signals of the main components of the carpet tufting machine are measured with a fiber laser vibrometer to identify the main noise sources. In the noise signal analysis, an adaptive mode decomposition method EEMD, a source number estimation method AIC, and an independent component analysis algorithm FastICA are combined to form a single channel blind source separation method EEMD-AIC-FastICA. The single channel blind source separation method can separate the single channel noise signal into several independent components (ICs). By comparing the time-frequency analysis results of the ICs and the vibration signals of main components, the main noise sources can be identified.

3. Noise Source Identification of the Carpet Tufting Machine

3.1. Structure of the Carpet Tufting Machine. A typical carpet tufting machine structure diagram is shown in Figure 4. The typical carpet tufting machine uses four-bar linkage based on eccentric mode to implement reciprocating motion of tufting needles and hooks [17].

3.2. Vibration Measurement and Analysis of the Main Components. Because there is a little prior knowledge about the main noise sources of the carpet tufting machine and the noise is generated by the vibration, the vibration signals of the main components of the carpet tufting machine are measured with a fiber laser vibrometer. The vibration test arrangement is shown in Figure 5 and the six main test positions are shown in Figure 6. The vibration signals of the main components are analyzed in the time domain, frequency domain, and time-frequency domain. The analysis results are shown in Figures 7–9.

3.3. Noise Signal Acquisition. A typical 4-meter-wide carpet tufting machine was chosen as a noise signal acquisition object. A BK 4961 microphone was located at a textile worker's standing area. The measuring position was 1.0 meter away from a carpet tufting machine, and the height was 1.6 meter. The sampling frequency was 51200 Hz, and the spindle motor rotation speed was 360 rpm. Figure 10 shows the noise acquisition arrangement and Figure 11 shows the time-domain map of one second of noise signal.

3.4. Noise Signal EEMD Decomposition. First, a single channel noise signal is decomposed using EEMD with the added white noise amplitude of 0.2 and the ensemble number 100 into 14 IMF components and an approximate residual. The result is shown in Figure 12. Combining the evaluation of the energy characteristic index and the correlation coefficient, IMF energy and the correlation coefficient with the original signal are calculated, respectively. The calculation results are illustrated in Table 1. From Table 1, the main components IMF1 to IMF 10 are retained for source number estimation, and other IMF components are removed to purify the noise signal.

3.5. Improved AIC Source Number Estimation. The covariance matrix of the IMF component matrix is calculated and then SVD is applied. The following ten eigenvalues can be obtained: 0.0576, 0.0542, 0.0291, 0.0207, 0.0147, 0.0096, 0.0092, 0.0054, 0.0031, and 0.0030. After eigenvalue calibration, the AIC values are shown in Figure 13. Because the smallest AIC value corresponds to $k = 4$, the estimated source number is 4.

3.6. Noise Source Separation Using FastICA. Because the result of source number estimation is 4, IMF5 to IMF8 are chosen for the next calculation according to Table 1.

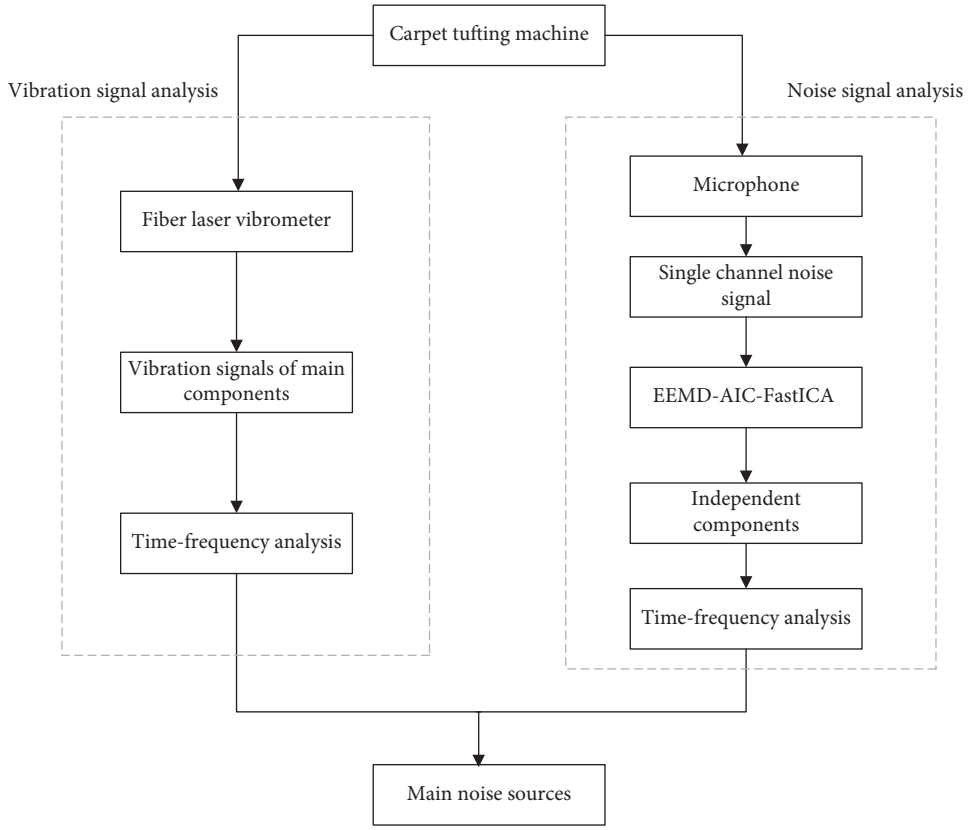

Figure 3: Schematic of the noise source identification of the carpet tufting machine.

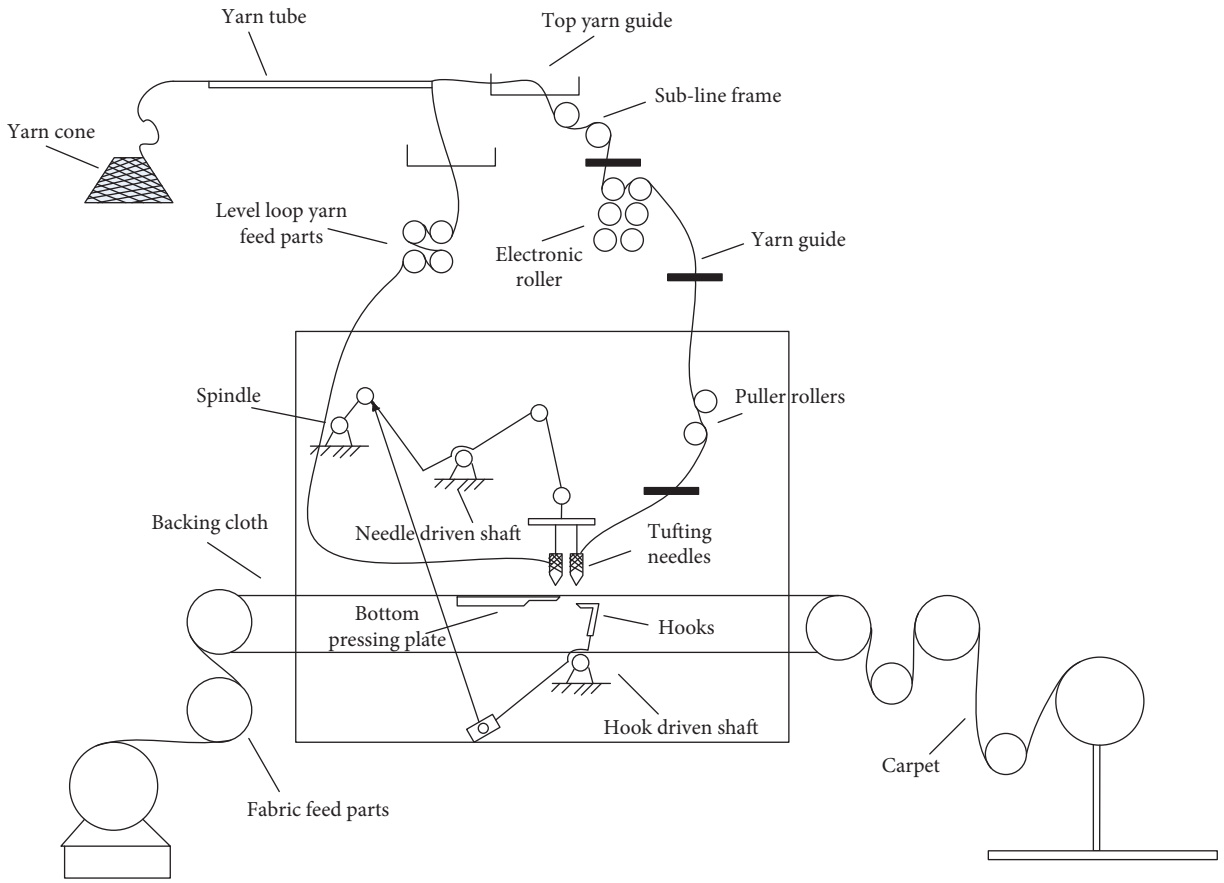

Figure 4: The structure diagram of a carpet tufting machine.

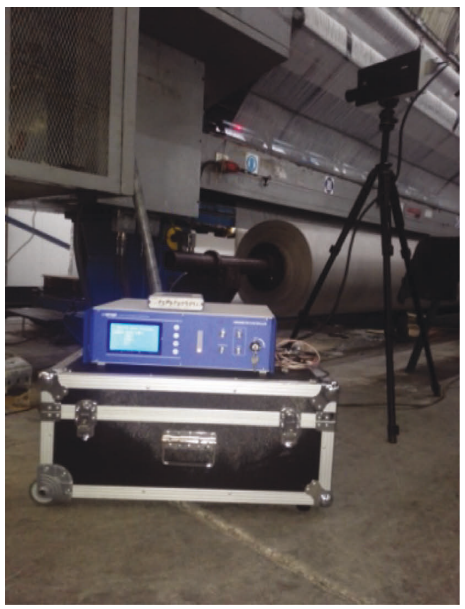

Figure 5: Vibration test arrangement.

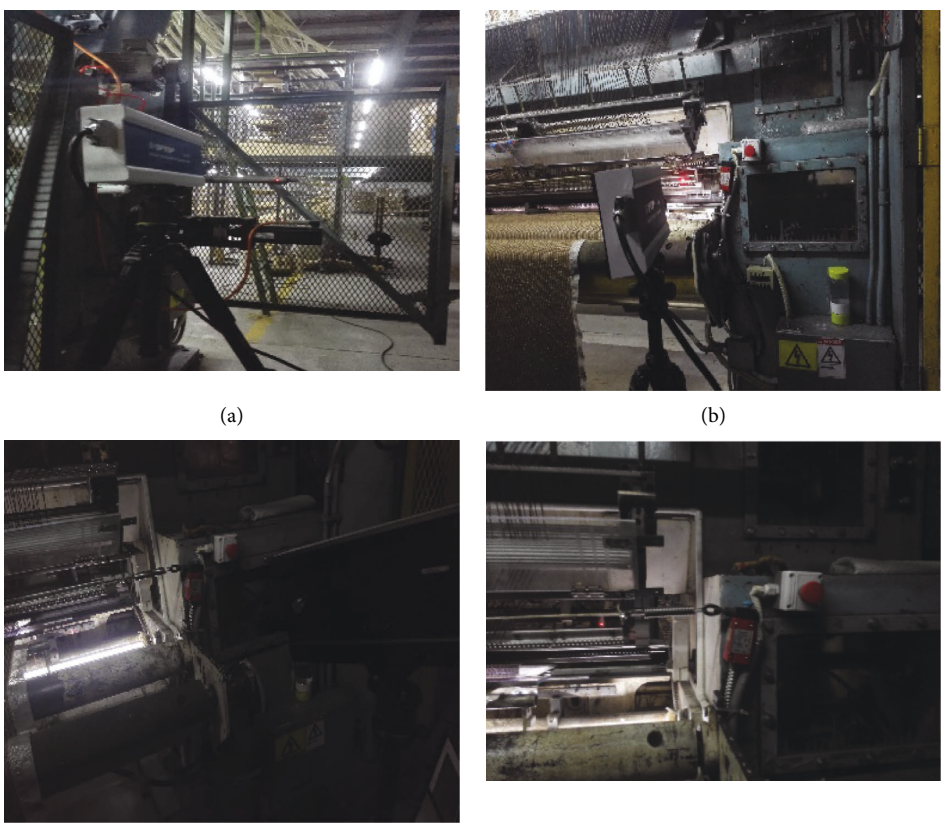

(a) (b) (c) (d)

Figure 6: Continued.

(e) (f)

Figure 6: Vibration test positions. (a) Motor spindle. (b) Needles. (c) Hook bed. (d) Linkage. (e) Hook driven shaft. (f) Bottom pressing plate.

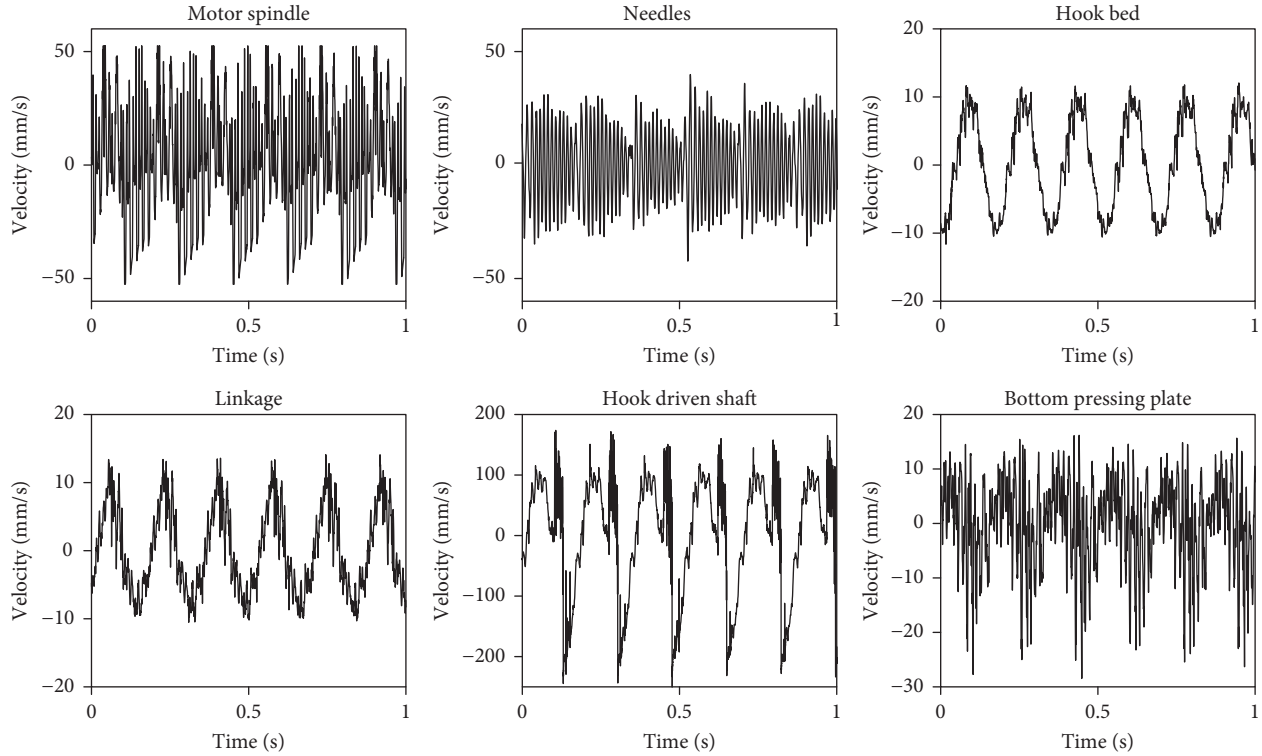

Figure 7: Time domain waveforms of vibration signals.

Furthermore, extracting the independent components from these IMFs, these IMFs and the original noise signal are combined to form a new signal group. The FastICA algorithm is applied to extract the independent components of the new signal group. The calculation results are shown in Figure 14. From Figure 14, these ICs may correspond to the four main noise sources.

3.7. Analysis of ICs. Although four ICs, which correspond to four main noise sources, have been separated, specific components producing these noises are still unknown. It is necessary to analyze the ICs in the time domain, frequency domain, and time-frequency domain. In Figure 14, the time domain waveforms of IC1 to IC4 have been shown. The spectra and spectrograms of ICs are shown, respectively in Figures 15 and 16.

3.8. Identification Results of the Main Noise Sources. Because the working rotation speed of the motor spindle is 360 rpm, almost all the main components in Figures 7–9 have a 6 Hz vibration frequency component, which is the fundamental frequency of the motor spindle. From the vibration analysis results in Figures 7–9, the motor spindle, the needles, and the hook driven shaft have high vibration

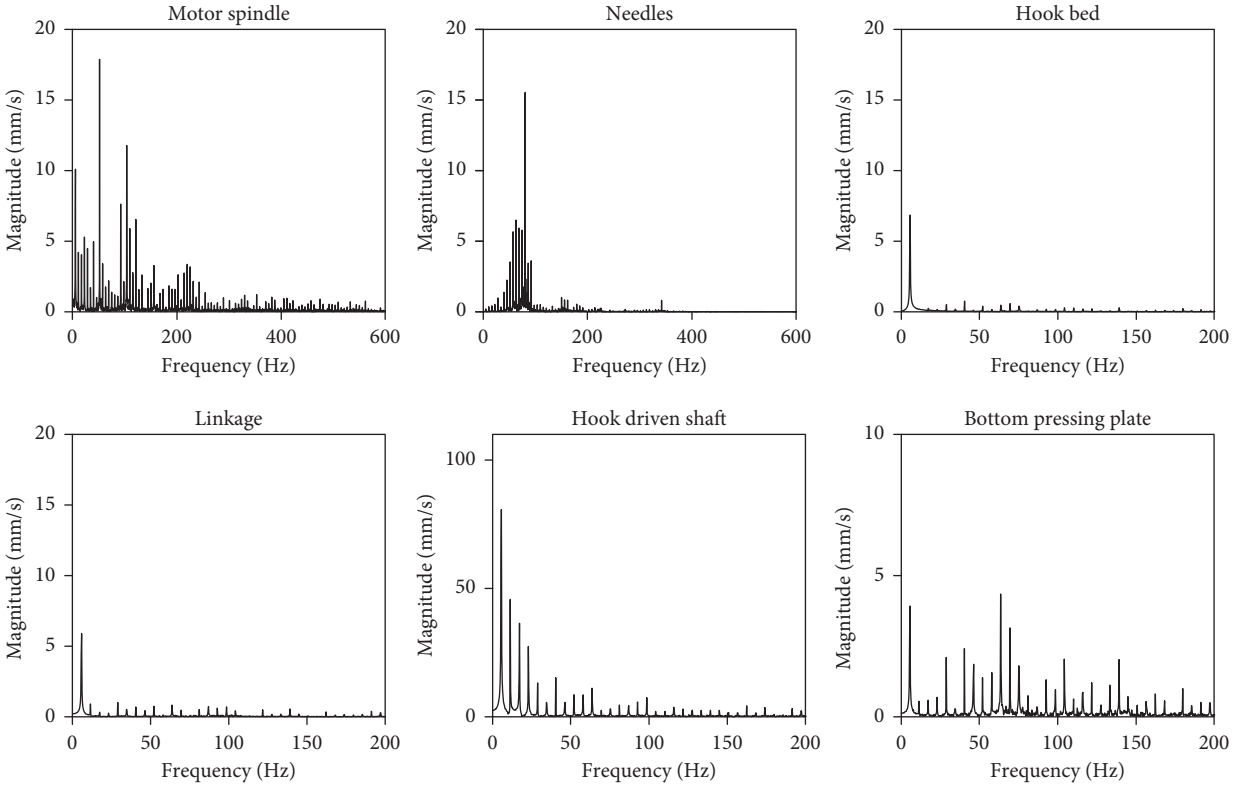

Figure 8: Spectra of vibration signals.

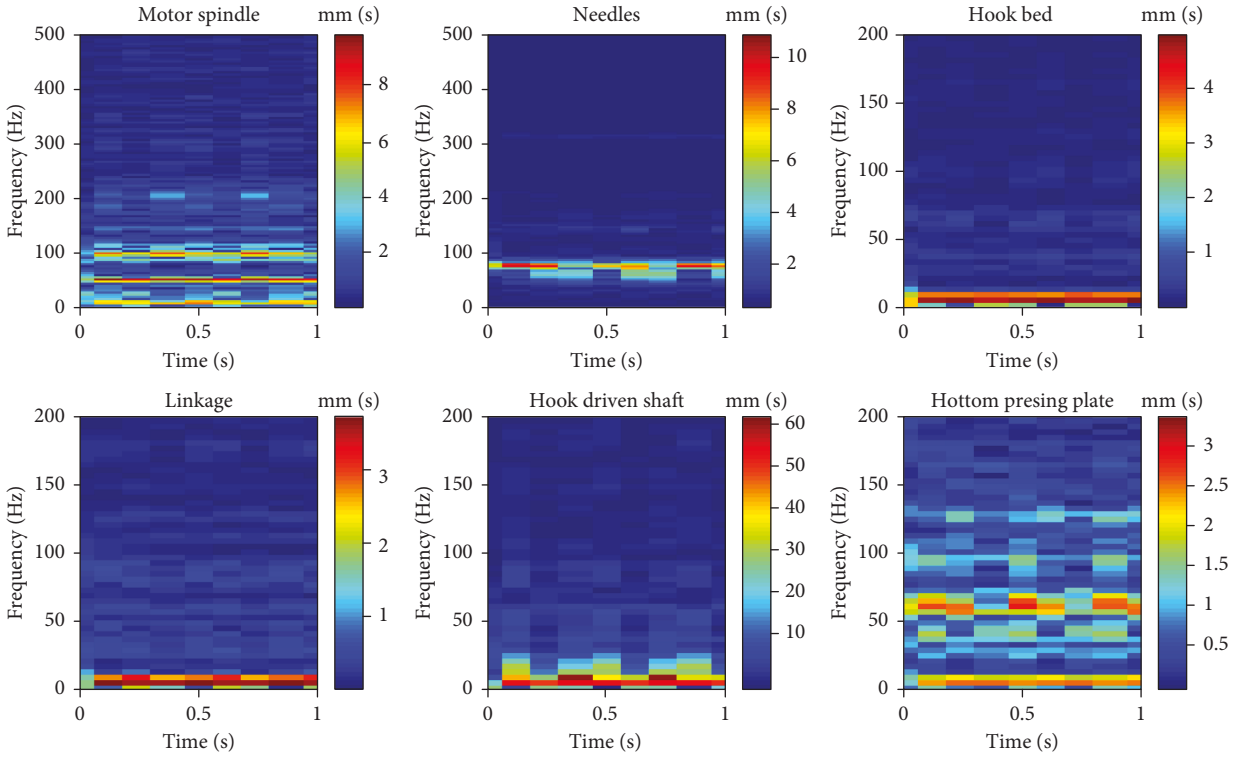

Figure 9: Spectrograms of vibration signals.

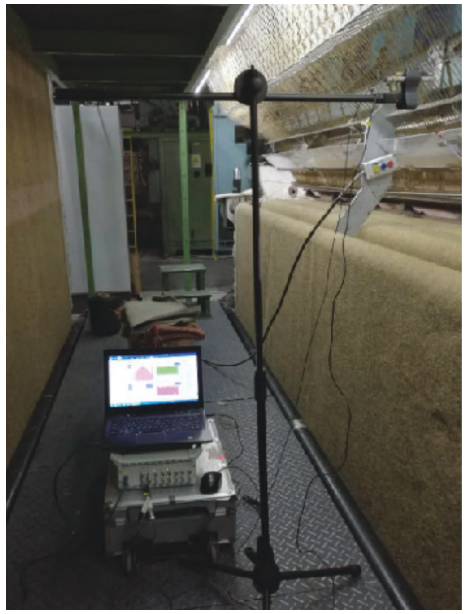

Figure 10: Noise acquisition arrangement.

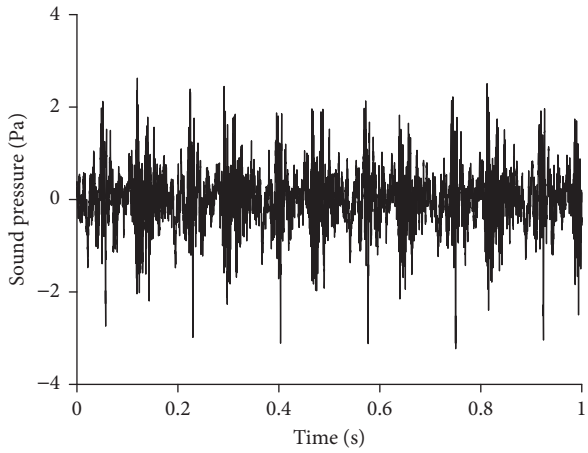

Figure 11: Time-domain map of the noise signal.

magnitude. Therefore, the main vibration sources are the motor spindle, the needles, the hooks, and the hook driven shaft.

According to the prior knowledge of the carpet tufting machine, the periodic impact of needles and hooks can produce periodic impulsive noise, and they should have similar noise spectra and spectrograms. From Figures 14–16, IC1 and IC2 have similar noise waveforms, spectra, and spectrograms, and they are periodic impulsive noise with many harmonics of fundamental frequency 6 Hz. The vibration spectrum and spectrogram of the needles in Figures 7–9 show the frequency components are harmonics of the fundamental frequency of 6 Hz. According to the discussion above, IC1 and IC2 should be the noise of needles and hooks. Because the stiffness of the needles is greater than the hooks' stiffness, the IC1 is the noise of the needles and the IC2 is the noise of the hooks.

Compared with the waveform, spectrum, and spectrogram of IC3 and IC4 with the waveform, spectrum, and spectrogram of the motor spindle and the hook driven shaft, their main frequency components are all harmonics of the fundamental frequency of 6 Hz. From Figures 7–9, the vibration frequency of the hook driven shaft is lower than the vibration frequency of the motor spindle. Moreover, the hook driven shaft should have a similar periodic impulsive noise with hooks. Therefore, IC3 is the noise of the hook driven shaft and IC4 is the noise of the motor spindle.

4. Discussion

The main contribution of this paper is the single channel blind source separation method based on EEMD-AIC-FastICA, and this method is applied in the noise source separation of the carpet tufting machine. In the literature

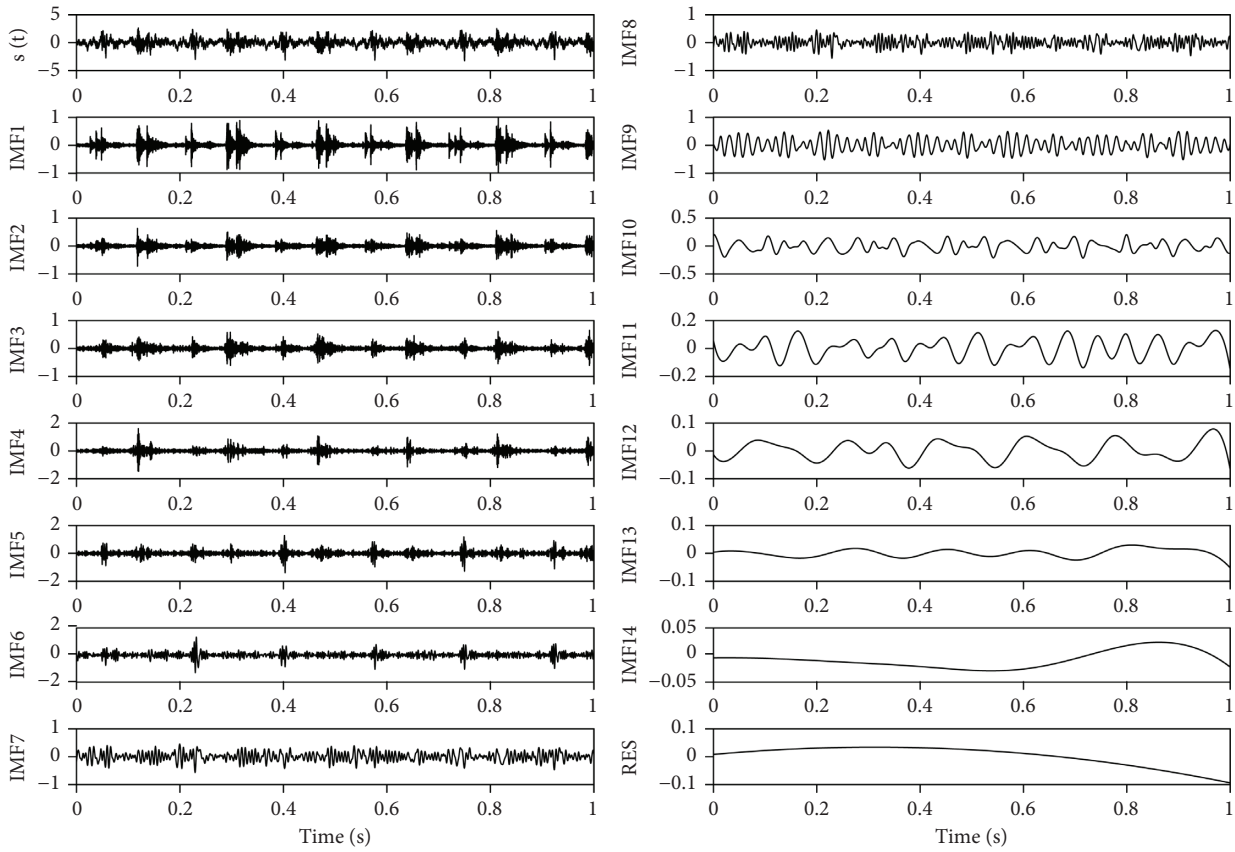

Figure 12: The result of EEMD decomposition.

Table 1: Calculation results of all IMF components.

IMF components	Correlation coefficient	Total energy/Pa^2
Original signal	1	16102
IMF 1	0.1864	457.1384
IMF 2	0.1732	197.4810
IMF 3	0.2222	266.4819
IMF 4	0.3987	1253.8
IMF 5	0.5535	1818.3
IMF 6	0.5746	1998.8
IMF 7	0.5046	1245.7
IMF 8	0.5067	2688.4
IMF 9	0.2580	424.8783
IMF 10	0.2096	299.5751
IMF 11	0.0948	55.4166
IMF 12	0.0378	10.5440
IMF 13	0.0004	15.8688
IMF 14	0.0047	3.6633
Residue	0.0052	65.1242

review of Section 1, references [5–7] used EEMD-RobustICA, VMD-RobustICA, and TVF-EMD-RobustICA to separate the noise sources of the engine noise, respectively. They all used an adaptive mode decomposition method. The first adaptive mode decomposition method was EMD, proposed in 1998, and then, many other similar methods were proposed, such as EEMD, VMD (variational mode decomposition) [18] and TVF-EMD (time varying filtering-empirical mode decomposition) [19]. Each adaptive mode decomposition method has some advantages and drawbacks, and is appropriate for different signals. In reference [5–7], they all used the RobustICA method. The RobustICA is similar with FastICA and it has better performance than the FastICA according to references [5–7]. In references [5–7], the main noise sources of the engine noise are known in advance, and the objective to evaluate the separation effect

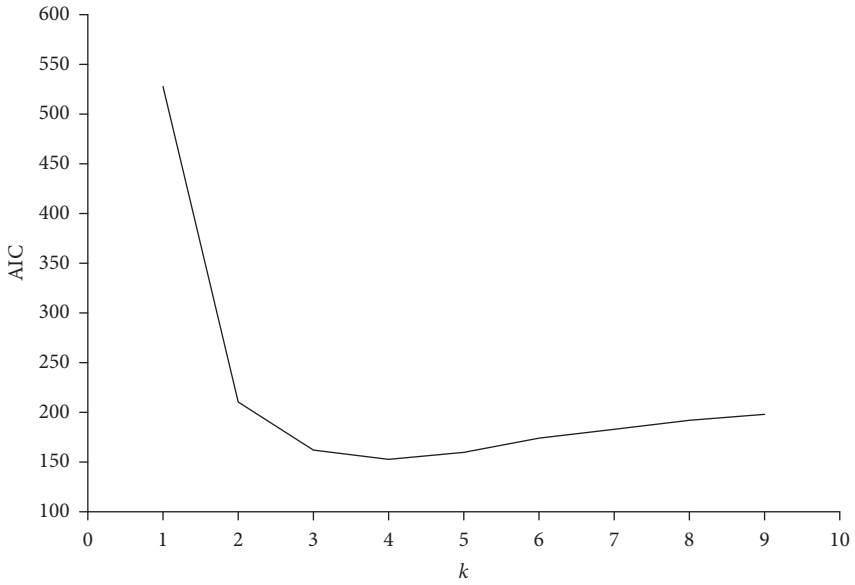

Figure 13: Calculation results of improved AIC.

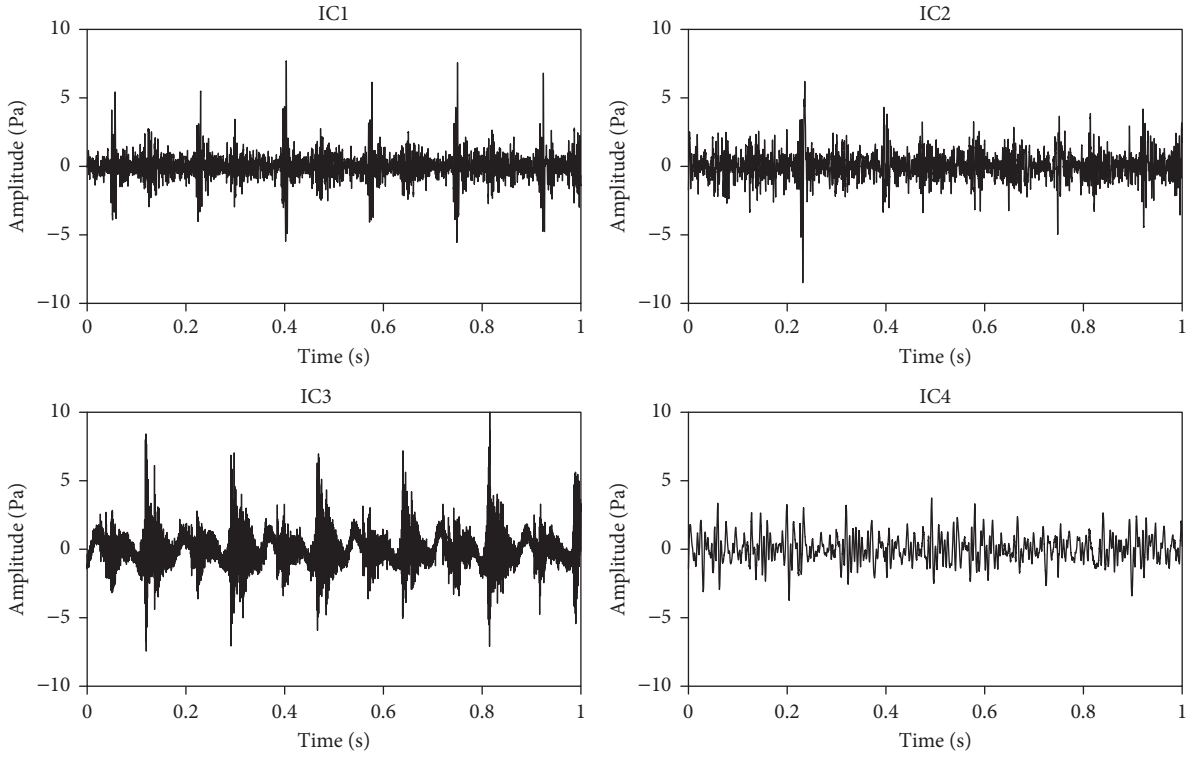

Figure 14: EEMD-AIC-FastICA separation results.

of their novel separation methods. However, the main sources of noise from the carpet tufting machine are unknown. The objective of this paper is to find a noise source identification method, and the single channel blind source separation is the most key step. Because the VMD method is needed to set the number of decomposition components, it is not appropriate for separating the noise in which the number of the noise sources is unknown. Because the TVF-EMD method decomposed 25 components for the same single channel noise of the carpet tufting machine, the decomposition number is too many and it is also inappropriate.

According to the discussion above, the EEMD-RobustICA method was chosen to compare with the EEMD-AIC-FastICA method, whose separation result is shown in Figure 14. The separation result of EEMD-RobustICA is shown

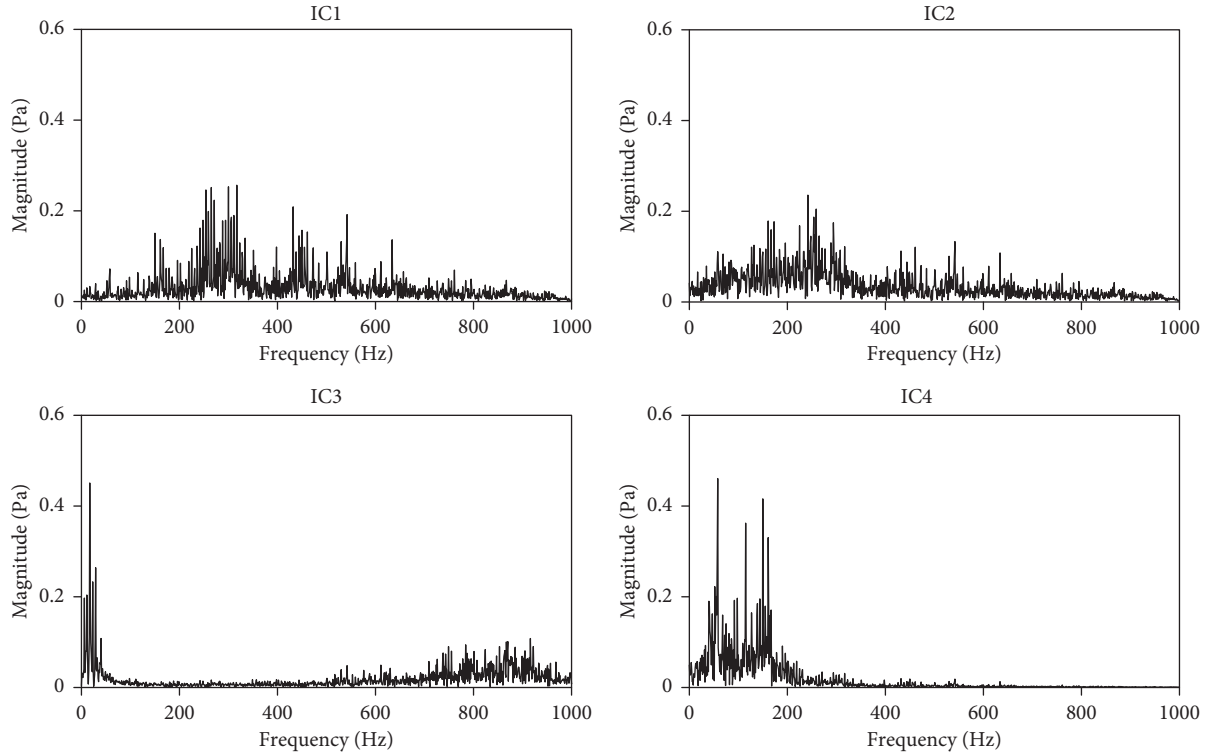

Figure 15: Spectra of IC1 to IC4.

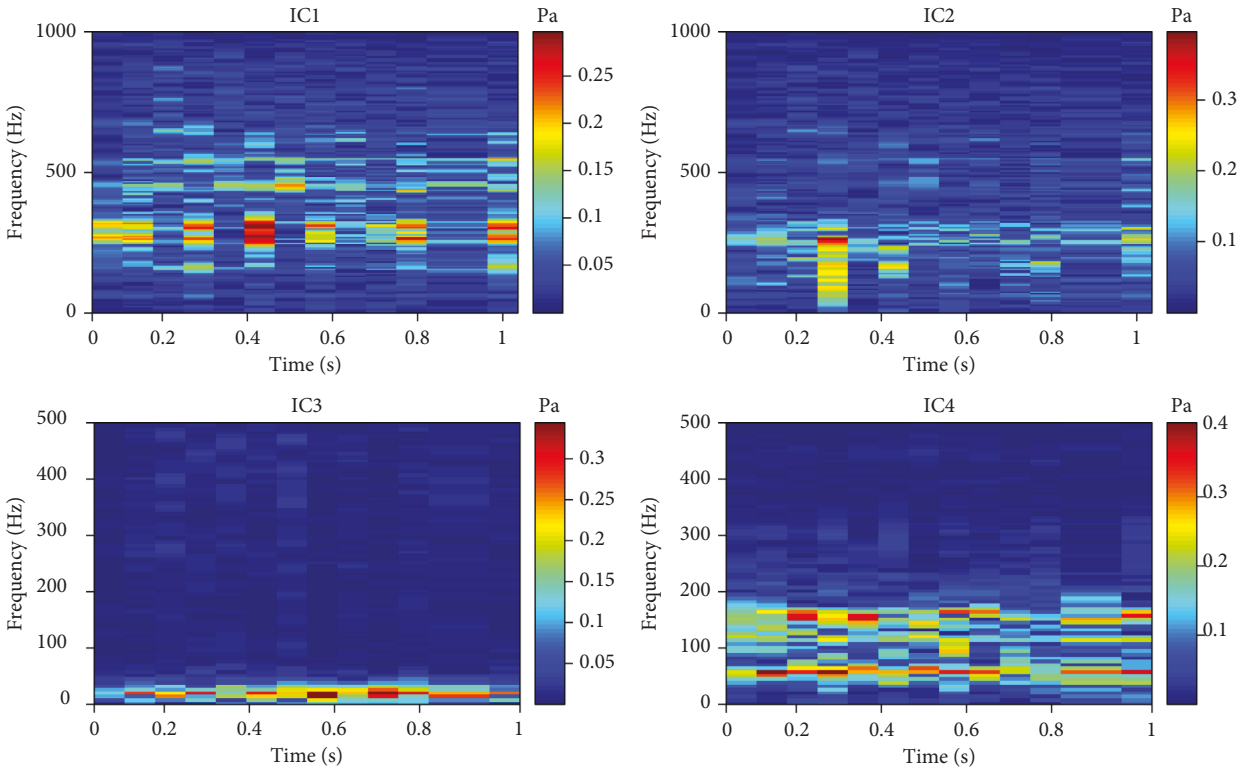

Figure 16: Spectrograms of IC1 to IC4.

in Figure 17. Compared with Figure 14 with Figure 17, there are only four independent components in Figure 14 while there are eleven independent components in Figure 17. Therefore, the EEMD-AIC-FastICA separation method is easier for the noise source identification with an unknown noise source number. There is an advantage to the EEMD-

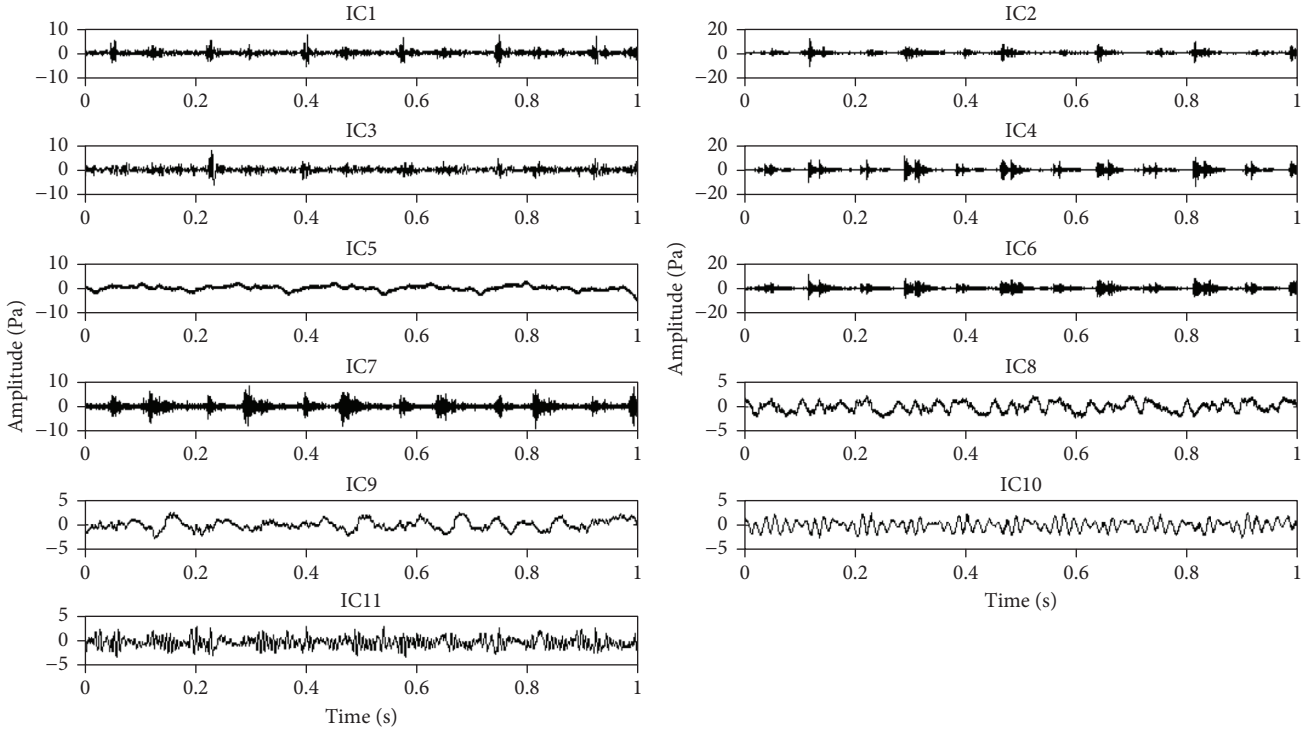

Figure 17: EEMD-RobustICA separation results.

RobustICA, which is more efficient in computation. However, the identification effect is more important for this paper's application.

5. Conclusions

In this paper, a single channel blind source separation method EEMD-AIC-FastICA is proposed and is applied in separating the main noise sources of the carpet tufting machine. The separation results are four ICs, which correspond to four main noise sources. According to the comparing discussion, EEMD-AIC-FastICA has a better separation effect for the noise source separation of the carpet tufting machine.

To identify the four main noise sources, vibration signals of the main components of the carpet tufting machine are measured with a fiber laser vibrometer. According to the time-frequency analysis of ICs and vibration signals, the four main noise sources are identified. IC1 is the noise of the needles, IC2 is the noise of the hooks, IC3 is the noise of the hook driven shaft, and IC4 is the noise of the motor spindle.

Research results show that the proposed method can effectively identify the main noise sources of the carpet tufting machine. The method which is proposed and used in this paper can provide theoretical support for the noise reduction plan of the carpet tufting machines and other similar textile machineries.

Data Availability

The MAT-file data of single channel noise signal and vibration signals of main components used to support the findings of this research are available from the corresponding author upon request.

Conflicts of Interest

The authors declare that they have no conflicts of interest.

Acknowledgments

This work was supported by the National Natural Science Foundation of China (No. 51675094) and the Fundamental Research Funds for the Central Universities (No. 2232016D3-27).

References

[1] *Ministry of Housing and Urban-Rural Development of the People's Republic of China, GB/T 50087-2013, Code for Design of Noise Control of Industrial Enterprises*, China Building Industry Press, Beijing, China, 2014.

[2] S. H. Chiu and C. P. Lu, "Noise separation of the yarn tension signal on twister using FastICA," *Mechanical Systems and Signal Processing*, vol. 19, no. 6, pp. 1326–1336, 2005.

[3] C. Servière, J. L. Lacoume, and M. El Badaoui, "Separation of combustion noise and piston-slap in diesel engine—Part II: separation of combustion noise and piston-slap using blind source separation methods," *Mechanical Systems and Signal Processing*, vol. 19, no. 6, pp. 1218–1229, 2005.

[4] X. Du, Z. Li, F. Bi, J. Zhang, X. Wang, and K. Shao, "Source separation of diesel engine vibration based on the empirical mode decomposition and independent component analysis," *Chinese Journal of Mechanical Engineering*, vol. 25, no. 3, pp. 557–563, 2012.

[5] F. Bi, L. Li, J. Zhang, and T. Ma, "Source identification of gasoline engine noise based on continuous wavelet transform and EEMD-RobustICA," *Applied Acoustics*, vol. 100, pp. 34–42, 2015.

[6] J. Yao, Y. Xiang, S. Qian, S. Wang, and S. Wu, "Noise source identification of diesel engine based on variational mode decomposition and robust independent component analysis," *Applied Acoustics*, vol. 116, pp. 184–194, 2017.

[7] J. Yao, Y. Xiang, S. Qian, and S. Wang, "Noise source separation of an internal combustion engine based on a single-channel algorithm," *Shock and Vibration*, vol. 2019, Article ID 1283263, 19 pages, 2019.

[8] X. Yang, Z. Ziyu, L. Angang, and S. Xiaowei, "Noise source identification method for a warp machine based on MEEMD_AIC," *Fibres and Textiles in Eastern Europe*, vol. 28, pp. 55–61, 2020.

[9] W. Haohui, S. Xiaowei, and X. Yang, "Noise source identification method for a carpet tufting machine based on CEEMDAN-AIC," *Shock and Vibration*, vol. 202113 pages, Article ID 5513062, 2021.

[10] N. E. Huang, Z. Shen, S. R. Long et al., "The empirical mode decomposition and the Hilbert spectrum for nonlinear and non-stationary time series analysis," *Proceedings of the Royal Society of London. Series A: Mathematical, Physical and Engineering Sciences*, vol. 454, pp. 903–995, 1971.

[11] Y. Lei, Z. He, and Y. Zi, "Application of the EEMD method to rotor fault diagnosis of rotating machinery," *Mechanical Systems and Signal Processing*, vol. 23, no. 4, pp. 1327–1338, 2009.

[12] Z. H. Wu and N. E. Huang, "Ensemble empirical mode decomposition: a noise assisted data analysis method," *Advances in Adaptive Data Analysis*, vol. 01, no. 01, pp. 1–41, 2009.

[13] N. Ma and J. T. Goh, "Efficient method to determine diagonal loading value," *Acoustics Speech and Signal Processing*, vol. 15, no. 4, pp. 341–344, 2005.

[14] A. Hyvarinen and E. Oja, "Independent component analysis: algorithms and applications," *Neural Networks*, vol. 13, no. 4-5, pp. 411–430, 2000.

[15] A. Hyvarinen and E. Oja, "A fast fixed-point algorithm for independent component analysis," *Neural Computation*, vol. 9, no. 7, pp. 1483–1492, 1997.

[16] W. Cheng, Z. Jia, X. Chen, and L. Gao, "Convolutive blind source separation in frequency domain with Kurtosis maximization by modified conjugate gradient," *Mechanical Systems and Signal Processing*, vol. 134, Article ID 106331,, 2019.

[17] X. Yang, S. Zhijun, M. Zhuo, S. Yize, and C. Guangfeng, "Research on yarn tension modeling in carpet tufting equipment system," *Journal of Manufacturing Science and Engineering*, vol. 133, no. 3, Article ID 031002, 2011.

[18] K. Dragomiretskiy and D. Zosso, "Variational mode decomposition," *IEEE Transactions on Signal Processing*, vol. 62, no. 3, pp. 531–544, 2014.

[19] H. Li, Z. Li, and W. Mo, "A time varying filter approach for empirical mode decomposition," *Signal Processing*, vol. 138, pp. 146–158, 2017.